Int J Thermophys (2009) 30:416–438
DOI 10.1007/s10765-007-0288-6

High-Temperature and Nonequilibrium Partition Function and Thermodynamic Data of Diatomic Molecules

Y. Babou · Ph. Rivière · M.-Y. Perrin · A. Soufiani

Received: 8 June 2007 / Accepted: 10 September 2007 / Published online: 13 November 2007

Abstract Accurate molecular partition functions are required to determine both thermodynamic properties for equilibrium and nonequilibrium flow field calculations, and energy level populations for radiative heat transfer in high enthalpy flows, for instance. Thermodynamic functions of diatomic molecules are computed in this study at high temperatures and for nonequilibrium media in the framework of multi-temperature models. Partition functions, average energies, and specific heats of N_2, N_2^+, NO, O_2, CN, C_2, CO, and CO^+ are calculated up to 50,000 K by direct summation over energy levels using recent and accurate spectroscopic data and dissociation energy values. Estimates are made for the error introduced by neglecting the highest considered electronic states. For nonequilibrium media, the sensitivity of the multi-temperature thermodynamic functions to different schemes for energy partitioning is discussed. In particular, the effects of vibration–rotation coupling are investigated. The tabulated results are available upon request.

Keywords Diatomic molecules · High temperature · Nonequilibrium · Partition function · Specific heat

1 Introduction

Accurate values of partition functions are required to calculate energy level populations (as input to radiative transfer calculations, for instance [1]), but they are also the starting point to derive thermodynamic data. The present work was motivated by the planned Martian exploration missions which require the prediction of heat fluxes, in particular radiative fluxes, and flow field calculations to characterize the entry phase. During this

Y. Babou · P. Rivière · M.-Y. Perrin (✉) · A. Soufiani
Laboratoire EM2C, CNRS UPR288, École Centrale Paris, 92295 Châtenay-Malabry Cedex, France
e-mail: Marie_Yvonne.Perrin@em2c.ecp.fr

entry phase, a shock wave is created in the front region which heats the gas to very high temperatures. Depending on the spacecraft trajectory and on the entry point, the shock layer can be in a nonequilibrium thermochemical state. A detailed microscopic description of the thermal nonequilibrium is still a prohibitive task, and a common simplification of this complex situation consists in using a two-temperature model [2–4]. In this model, the medium is characterized by two temperatures, T_r and T_v, through the assumption of a Boltzmann distribution for rotation and a Maxwell distribution for translation both at T_r, and a unique Boltzmann distribution for electronic and vibrational energy levels at T_v.

The main sources for high-temperature equilibrium thermodynamic properties of the considered diatomic molecules are the JANAF tables (limited to 6,000 K [5]), the NASA tables [6] based on the data of Gurvich et al. [7,8] which reach 20,000 K, and more recently the ESA tables [9] for temperatures as high as 50,000 K. For the nonequilibrium case, to the best of our knowledge, the only study going beyond the approximation of the rigid rotor has been carried out by Jaffe [10] for O_2, NO, and N_2.

In this study, starting from selected up-to-date spectroscopic data, we computed local thermodynamic equilibrium (LTE) internal partition functions, internal energies and internal specific heats for N_2, N_2^+, NO, O_2, CN, C_2, CO, and CO^+ molecules for temperatures ranging from 1,000 to 50,000 K. In the framework of a two-temperature model for thermal nonequilibrium media, the vibration–rotation separability problem is investigated by analyzing the impact of the strategy used for the internal energy partitioning on non-LTE internal specific heats.

In Sect. 2.1, we describe the details of the methodology which was adopted to calculate LTE partition functions. The LTE results in terms of internal partition function, internal average energy, and internal specific heat are then presented and discussed in Sect. 2.2. The methodology is extended to non-LTE media in Sect. 3.1. Section 3.2 is devoted to non-LTE results with a two-temperature description.

2 Internal Partition and Thermodynamic Functions at Equilibrium

2.1 Calculation Methods and Selected Data

In the framework of statistical mechanics, the internal partition function of a molecule or an atom can be written in its most general form as

$$Q_{\text{int}}(T) = \sum_{i_c} g_{i_c} \exp\left(-\frac{\mathcal{E}_{i_c} - \mathcal{E}_0}{k_B T}\right), \tag{1}$$

where $\mathcal{E}_{i_c}$ is the energy of the i_c-th quantum configuration, $\mathcal{E}_0$ is the energy of the lowest energy level, and g_{i_c} is the degeneracy of the i_c-th configuration. The summation is over all possible energy levels available to the system.

Neglecting the hyperfine structure and averaging nuclear spin effects for homonuclear molecules at the elevated temperatures considered here, the diatomic internal

partition function is given by the following expression:

$$Q_{\mathrm{int}}(T) = \frac{1}{\sigma} \sum_{n}^{n_{\max}} \sum_{v}^{v_{\max}} \sum_{i}^{i_{\max}} \sum_{J}^{J_{\max}} \sum_{p}^{p_{\max}} (2J+1) e^{-hc \frac{E_{n,v,i,J,p} - \mathcal{E}_0}{k_{\mathrm{B}} T}}, \tag{2}$$

where $\sigma = 1$ for heteronuclear molecules and $\sigma = 2$ for homonuclear molecules (in order to account for average nuclear spin statistical weight). $E_{n,v,i,J,p}$ is the energy of the quantum configuration characterized by the pentuplet (n, v, i, J, p). The number p allows one to distinguish Λ-doubling components, J is the rotational quantum number, i allows one to distinguish spin-multiplet components, v is the vibrational quantum number, and n is related to the electronic level. $\mathcal{E}_0$ is the energy of the diatomic molecule in its lowest energy configuration.

By assuming that the energy variation of $E_{e,v,i,J,p}$ with i and p has no influence, Eq. 2 reduces to a more simple expression where Λ-doubling and fine structure are not resolved:

$$Q_{\mathrm{int}}(T) = \frac{1}{\sigma} \sum_{n}^{n_{\max}} (2 - \delta_{\Lambda,0})(2S+1) \sum_{v}^{v_{\max}} \sum_{J}^{J_{\max}} (2J+1) e^{-hc \frac{E_{n,v,J} - \mathcal{E}_0}{k_{\mathrm{B}} T}}. \tag{3}$$

In this expression, S and Λ are the quantum numbers associated with the electronic spin angular momentum, and with the projection of the electronic orbital angular momentum, respectively. Neglecting nuclear hyperfine structure and Λ-doubling causes insignificant errors for the partition function in the considered temperature range. The multiplet structure contribution can be non-negligible for species with large spin-orbit coupling constants at low temperatures. A contribution of a few percent is observed for NO below 3,000 K (see Sect. 2.2).

The total energy $E_{n,v,J}$ of the diatomic molecule in the level characterized by the triplet (n, v, J) is expressed as the sum of an electronic excitation energy, a vibrational energy, and a rotational contribution depending explicitly on v:

$$E_{n,v,J} = E_{\mathrm{el}}(n) + E_{\mathrm{vib}}(n, v) + E_{\mathrm{rot}}(n, v, J). \tag{4}$$

The electronic excitation energy $E_{\mathrm{el}}(n)$ is referenced to the electronic ground state (i.e., $E_{\mathrm{el}}(n)$ is equal to the difference between the minima of the potential energy curves of the electronic level n and the electronic ground state). The vibrational energy $E_{\mathrm{vib}}(n, v)$ of the level v in the electronic state n is referenced to the electronic energy $E_{\mathrm{el}}(n)$. $\mathcal{E}_0$ is equal to the vibrational energy of the lowest level. It is given by

$$\mathcal{E}_0 = E_{0,0,0} = E_{\mathrm{el}}(0) + E_{\mathrm{vib}}(0, 0) + E_{\mathrm{rot}}(0, 0, 0) = E_{\mathrm{vib}}(0, 0). \tag{5}$$

Approximate methods, such as rigid rotor and harmonic oscillator approximations and summation limits extending to infinity, are inadequate at high temperatures; the partition functions for diatomic molecules should be set up by direct numerical summation over all vibration–rotation energy levels for all bound electronic states. The difficulties associated with the direct numerical summation are related to the knowledge of energy levels and to the definition of appropriate cutoff criteria. Previous works have proposed

different strategies [7,8,10–12]. The chosen approach follows from that developed in [11].

The calculation of the energy $E_{\mathrm{el}}(n)$, $E_{\mathrm{vib}}(n, v)$, $E_{\mathrm{rot}}(n, v, J)$ is based on the usual spectroscopic constants and energy expansions as follows:

$$E_{\mathrm{el}}(n) = T_e, \tag{6}$$

$$\begin{aligned} E_{\mathrm{vib}}(n, v) = {} & \omega_e \left(v + \frac{1}{2}\right) - \omega_e x_e \left(v + \frac{1}{2}\right)^2 + \omega_e y_e \left(v + \frac{1}{2}\right)^3 \\ & + \omega_e z_e \left(v + \frac{1}{2}\right)^4 + \omega_e a_e \left(v + \frac{1}{2}\right)^5 + \omega_e b_e \left(v + \frac{1}{2}\right)^6 \\ & + \omega_e c_e \left(v + \frac{1}{2}\right)^7 + \omega_e d_e \left(v + \frac{1}{2}\right)^8 + \omega_e e_e \left(v + \frac{1}{2}\right)^9, \end{aligned} \tag{7}$$

$$\begin{aligned} E_{\mathrm{rot}}(n, v, J) = {} & B_v J(J+1) - D_v (J(J+1))^2 \\ = {} & B_e (J(J+1)) - \alpha_e \left(v + \frac{1}{2}\right) J(J+1) + \gamma_e \left(v + \frac{1}{2}\right)^2 J(J+1) \\ & + \delta_e \left(v + \frac{1}{2}\right)^3 J(J+1) + \epsilon_e \left(v + \frac{1}{2}\right)^4 J(J+1) \\ & + \xi_e \left(v + \frac{1}{2}\right)^5 J(J+1) \\ & + \eta_e \left(v + \frac{1}{2}\right)^6 J(J+1) + \theta_e \left(v + \frac{1}{2}\right)^7 J(J+1) \\ & - D_e (J(J+1))^2 - \beta_e \left(v + \frac{1}{2}\right) (J(J+1))^2 \\ & - g_e \left(v + \frac{1}{2}\right)^2 (J(J+1))^2 \\ & - h_e \left(v + \frac{1}{2}\right)^3 (J(J+1))^2 - k_e \left(v + \frac{1}{2}\right)^4 (J(J+1))^2. \end{aligned} \tag{8}$$

The electronic level energy T_e and the spectroscopic constants ω_e, $\omega_e x_e$, ... and B_e, D_e, ... are taken from the literature. They are generally determined by fitting the previous expressions to experimental spectroscopic data or ab-initio calculations. A careful analysis of the available data has been performed to select the most precise data covering the maximum range in terms of v and J values. The constants ω_e and B_e are almost always tabulated except for a few ab-initio states for which we impose values close to those of a neighbor state. If one of the other constants is lacking, it is taken equal to 0 except D_e and β_e which are calculated according to [13]

$$D_e = \frac{4B_e^3}{\omega_e^2}, \tag{9}$$

$$\beta_e = D_e \left(\frac{8\omega_e x_e}{\omega_e} - \frac{5\alpha_e}{B_e} - \frac{\alpha_e^2 \omega_e}{24 B_e^3} \right). \tag{10}$$

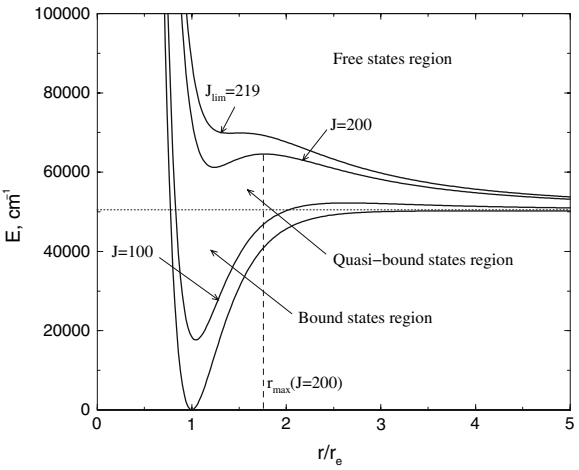

Fig. 1 Potential curves $V_J(r)$ at different J for $X^1\Sigma_g^+$ state of the C_2 molecule

The summation must include all vibrational states up to the dissociation limit. For a given electronic level n, we consider all values of v for which the following cutoff criterion is satisfied:

$$E_{\text{vib}}(n, v) < E_{\text{diss}}(n) \tag{11}$$

where $E_{\text{diss}}(n)$ is the rotationless ($J = 0$) dissociation energy of the nth electronic level, referenced to the minimum of its potential energy curve. As a rule, the rotationless dissociation energy is determined on the basis of the electronic level energy T_e and the energies of the dissociation products. For a few electronic states, the extrapolation of $E_{\text{vib}}(n, v)$ expressions leads to non-convergence behavior towards the dissociation limit. In this case, $v_{\max}$ is determined as the last vibrational level before the derivative $\left(\frac{\partial E_{\text{vib}}(n,v)}{\partial v}\right)$ changes its sign. The effect was limited for the present species; otherwise more sophisticated models could be used [7].

For a given electronic state and for each vibrational quantum number $v \leq v_{\max}$, we consider all the rotational levels below the energy of the dissociation limit of the rotating molecule. The allowed (v,J) values are defined from the condition:

$$E_{\text{vib}}(n, v) + E_{\text{rot}}(n, v, J) \leq V_J(r_{\max}(J)), \tag{12}$$

where $V_J(r)$ is the effective potential energy of the rotating molecule and $r_{\max}(J)$ is the local maximum position of the $V_J(r)$ curve. In this way, we take into account all bound and quasi-bound states. An example of bound, quasi-bound, and free states regions is shown on Fig. 1 for the ground electronic state of C_2. We assume that the effective potential energy $V_J(r)$ is the sum of a Morse potential and the centrifugal potential:

$$V_J(r) = E_{\text{diss}}(1 - e^{-2\beta\frac{r-r_e}{r_e}})^2 + B_e\left(\frac{r_e}{r}\right)^2 J(J+1), \tag{13}$$

where r_e is the equilibrium distance corresponding to the minimum value of the energy and β is a constant derived from [13]

$$\beta = \frac{\omega_e}{4(B_e E_{\text{diss}})^{\frac{1}{2}}}. \tag{14}$$

The J_{lim} value, corresponding to the potential curve separating free states region from bound and possible quasi-bound states regions (cf. Fig. 1), is determined from the conditions:

$$\begin{aligned} \text{for all } r, \quad & \frac{\partial V_{J_{\text{lim}}+1}(r)}{\partial r} \leq 0, \\ \text{there exists one } r \geq r_e \text{ such that } \quad & \frac{\partial V_{J_{\text{lim}}}(r)}{\partial r} > 0. \end{aligned} \tag{15}$$

For each $J < J_{\text{lim}}$, the outer position of the bound state region, $r_{\max}(J)$ is determined by:

$$\left(\frac{\partial V_J(r)}{\partial r}\right)_{r_{\max}(J)} = 0, \tag{16}$$

$$\left(\frac{\partial^2 V_J(r)}{\partial r^2}\right)_{r_{\max}(J)} < 0. \tag{17}$$

Finally, the condition in Eq. 12 allows one to define a $J_{\max}$ value for each v. In addition, for a few states, we had to impose the condition that the function $J_{\max}(v)$ be a decreasing function with v by implementing the constraint:

$$J_{\max}(v+1) \leq J_{\max}(v). \tag{18}$$

The reliability of $J_{\max}$ and $v_{\max}$ values depends on possible uncertainties in the dissociation energy and on the quality of extrapolated energies. This latter point is difficult to quantify; a comparison with results based on different energy expansions can help to evaluate the possible variations.

The considered electronic states, as well as the corresponding spectroscopic constants, are presented in Appendix A. For $T = 20{,}000$ K, for instance, the energy of the upper considered electronic state ranges between 4.5 and 6.4 in units of $k_B T$ for the different molecules (4.5 for CO^+ and 6.4 for N_2). All observed states up to this electronic limit have been considered. We have also taken into account non-observed but theoretically predicted states. To have an idea of the inaccuracy linked to these limitations, we have calculated the percentage contributions to Q_{int}, E_{int}, and $C_{p,\text{int}}$ (the derivation of these last two quantities is given in Sect. 2.2) of the last electronic state taken into account in our calculations. These contributions are given in Table 1 for 30,000 and 50,000 K. For all the considered molecules, the contribution of the $n_{\max}$-th level listed in Appendix A increases with the temperature and remains lower than 5% at 50,000 K. As E_{int} and $C_{p,\text{int}}$ are obtained from $Q_{\text{int}}(T)$ temperature derivatives, there is no direct correlation between the contribution of one given electronic state

Table 1 Percentage contributions to $Q_{\text{int}}(T)$, $E_{\text{int}}(T)$, and $C_{p,\text{int}}(T)$ of the $n_{\max}$-th electronic state at 30,000 K and 50,000 K

Molecule	O_2	N_2^+	N_2	NO	CN	C_2	CO^+	CO
$n_{\max}$	21	16	11	16	16	20	8	9
Q_{int}(30,000 K)	0.25	0.77	0.45	0.67	0.63	0.25	0.33	3.8
Q_{int}(50,000 K)	0.73	1.1	0.67	1.15	1.16	0.80	0.39	4.8
E_{int}(30,000 K)	0.43	0.29	0.17	0.49	0.46	0.43	0.07	0.97
E_{int}(50,000 K)	0.94	0.25	0.12	0.45	0.62	1.1	0.04	0.58
$C_{p,int}$(30,000 K)	2.9	0.17	−0.021	0.78	1.5	3.5	−0.19	−1.7
$C_{p,int}$(50,000 K)	4.74	−0.22	−0.36	−0.3	2.0	6.4	−0.33	−3.21

to the partition function and its contribution to E_{int} and $C_{p,\text{int}}$ when the temperature increases. Indeed, as can be seen for instance for the CO molecule, the inclusion of the last electronic state increases the internal partition function by 3.8% at 30,000 K and 4.8% at 50,000 K, whereas its relative contribution to E_{int} decreases with T. Table 1 shows that neglecting possible additional high-lying electronic states would probably not modify in a critical way the values of Q_{int}, E_{int}, and $C_{p,\text{int}}$ even at high temperatures.

2.2 Results at Equilibrium

Having determined the internal partition functions Q_{int}, we can calculate internal thermodynamic functions, such as the internal contribution E_{int} to the average energy or the internal specific heat $C_{p,\text{int}}$. For 1 mol of an ideal gas at the equilibrium temperature T, the average internal energy and internal specific heat are calculated from the first and second derivatives of Q_{int} as follows:

$$E_{\text{int}}(T) = RT^2 \left(\frac{\partial \ln Q_{\text{int}}(T)}{\partial T} \right), \tag{19}$$

$$C_{p,\text{int}}(T) = \frac{\partial E_{\text{int}}(T)}{\partial T}, \tag{20}$$

where R is the universal gas constant.

The average energy and specific heat values have been calculated by a numerical differentiation of the partition function according to

$$E_{\text{int}}(T) = RT^2 \left(\frac{\ln Q_{\text{int}}(T + \delta T) - \ln Q_{\text{int}}(T - \delta T)}{2\delta T} \right), \tag{21}$$

$$C_{p,\text{int}}(T) = \frac{E_{\text{int}}(T + \delta T) - E_{\text{int}}(T - \delta T)}{2\delta T}. \tag{22}$$

The numerical values were found to be insensitive to δT for values lower than 20 K. The average energy $E_{\text{int}}(T)$ and specific heat $C_{p,\text{int}}(T)$ were computed with $\delta T = 10$ K.

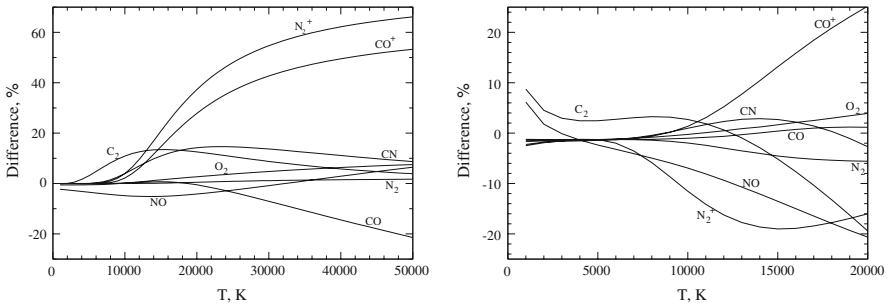

Fig. 2 Percentage difference between present partition functions and results from [9] (*left*) and from [6] (*right*)

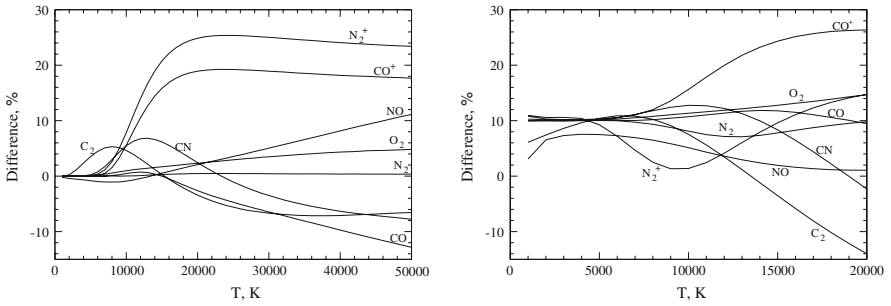

Fig. 3 Percentage difference between present internal average energies and results from [9] (*left*) and from [6] (*right*)

In the following, comparisons with ESA tables [9] and NASA data [6] are done in terms of relative differences between our results and the other data:

$$100 \times \left(\frac{X(T) - X^{\mathrm{ESA,NASA}}(T)}{X(T)} \right), \tag{23}$$

where X designates Q_{int}, E_{int}, or $C_{p,\mathrm{int}}$. Comparisons with ESA and NASA data are shown on Figs. 2, 3, and 4 for Q_{int}, E_{int}, and $C_{p,\mathrm{int}}$, respectively.

The spectroscopic data used for the ESA tables come from Huber and Herzberg [14]. In comparison, Our selected data are more detailed for many electronic states and more exhaustive for very high temperatures. On the other hand, Gurvich et al. [7,8] have provided a remarkable study on thermodynamic data. They have collected the widest set of spectroscopic data, developed sophisticated extrapolation methods for low-lying electronic states, and deeply analyzed the possible errors. Due to the lack of spectroscopic data for many high-lying electronic states, they made an important approximation to compute the contribution of high energy electronic states; indeed, they assumed the same rotation–vibration structure for these states as for the ground state or for the last well known electronic state. In our calculations, we benefit from recent studies that allowed us to eliminate this approximation.

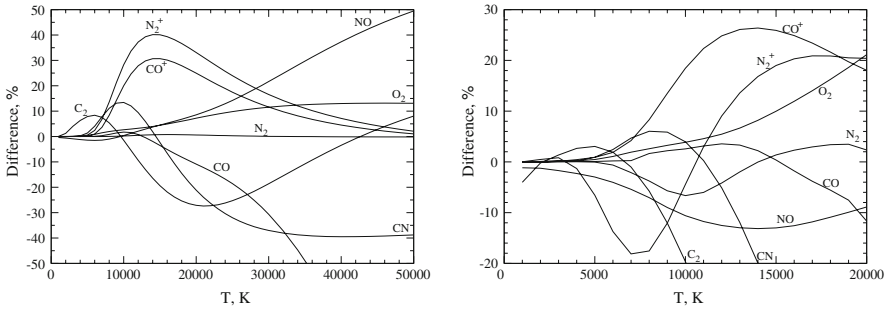

Fig. 4 Percentage difference between present internal specific heats and results from [9] (*left*) and from [6] (*right*)

For the most studied molecules, namely O_2, N_2, and CO, our calculated partition functions are in excellent agreement with both the NASA and ESA values up to 20,000 K. The differences are limited to about 5%. The agreement is also satisfactory for the CN molecule. The differences are generally much higher for less studied molecules. For N_2^+ at high temperature, our partition function, involving 16 electronic states, is higher than the ESA values, which are based on only six electronic states, but smaller than the NASA partition function. The latter contains some additional electronic states which have been theoretically predicted but not observed. Moreover, the rotation–vibration structure is described precisely for only the four lowest states in [7,8]. For NO, there is good agreement between our calculations and ESA results. The differences with the NASA results are quite large at both low and high temperatures. Below 3,000 K, these differences are due to spin splitting effects which are not taken into account in our calculations. However, at high temperature, we consider the same number of electronic states as in [7,8] and the difference is probably due to the approximate treatment of vibration and rotation for high-lying electronic states in Gurvich's predictions. The C_2 molecule is probably the most controversial among the molecules considered here. Comparisons with the NASA data show a discrepancy of 10% at low temperatures. We found no satisfactory explanation for this behavior, although successful comparisons with the JANAF [5] tables up to 6,000 K (not shown here) suggest that the NASA values should be reinvestigated at low temperatures. The differences at high temperature are due to many intermediate electronic states which are not well known. Finally, our predictions for CO^+ at high temperature are significantly higher than both ESA and NASA values. This is the result of the inclusion in our calculations of several intermediate states that have been recently investigated [15].

The relative differences between internal energies, shown on Fig. 3, are in the range $\pm 10\%$ up to 20,000 K, except for CO^+ and C_2 when comparisons are made with [6], and except for CO^+ and N_2^+ when they are made with [9]. As the internal specific heats are computed from the derivative of the internal energy with respect to the temperature, higher differences are generally observed for this last quantity (see Fig. 4).

The comparisons made above show that important discrepancies may appear among different sources of thermodynamic data for diatomic molecules at high temperature, depending on the cutoff and extrapolation criteria adopted for the electronic,

vibrational, and rotational levels. A better knowledge of fundamental spectroscopic data, particularly for high-lying electronic states, will reduce the uncertainties.

3 Non-LTE Partition and Thermodynamic Functions

For practical computation of nonequilibrium entry flows, a commonly used model [2–4] assumes that the flow can be described by two temperatures, T_r and T_v, by assuming a Boltzmann distribution for rotation and a Maxwell distribution for translation, both at T_r, and a unique Boltzmann distribution for electronic and vibrational energy levels at T_v. It is not the purpose of the present work to discuss the validity of this model, but the objective is to develop and discuss some models for partition and thermodynamic functions that are consistent with this two-temperature description.

3.1 Two-Temperature Formulation

The internal energy, given by Eq. 4, can be written as

$$E_{n,v,J} = E_\mathrm{el}(n) + E_\mathrm{vib}(n, v) + \bar{E}_\mathrm{rot}(n, J) + E_\mathrm{inter}(n, v, J), \tag{24}$$

where, for a given n, $E_\mathrm{vib}(n, v)$ is the part of the energy depending exclusively on v, $\bar{E}_\mathrm{rot}(n, J)$ is the part of $E_\mathrm{rot}(n, v, J)$ depending exclusively on J, and $E_\mathrm{inter}(n, v, J)$ is the vibration–rotation coupling term. The contribution of this last term is small at low temperature but cannot be neglected at high temperatures. Practically, two limiting cases are defined where $E_\mathrm{inter}(n, v, J)$ is assigned fully either to the vibrational contribution or to the rotational contribution. In these two limiting cases, the two-temperature partition function is expressed as [10]

$$\begin{aligned} Q_\mathrm{int}(T_\mathrm{v}, T_\mathrm{r}) = {} & \frac{1}{\sigma}\sum_{n=0}^{n_\mathrm{max}}(2-\delta_{\Lambda,0})(2S+1)e^{-hc\frac{E_{el}(n)}{k_\mathrm{B}T_\mathrm{v}}} \\ & \times \sum_{v=0}^{v_\mathrm{max}} e^{-hc\frac{E_\mathrm{vib}(n,v)-\mathcal{E}_0}{k_\mathrm{B}T_\mathrm{v}}} \sum_{J=0}^{J_\mathrm{max}}(2J+1)e^{-hc\frac{\bar{E}_\mathrm{rot}(n,J)+E_\mathrm{inter}(n,v,J)}{k_\mathrm{B}T_\mathrm{r}}}, \end{aligned} \tag{25}$$

or

$$\begin{aligned} Q_\mathrm{int}(T_\mathrm{v}, T_\mathrm{r}) = {} & \frac{1}{\sigma}\sum_{n=0}^{n_\mathrm{max}}(2-\delta_{\Lambda,0})(2S+1)e^{-hc\frac{E_{el}(n)}{k_\mathrm{B}T_\mathrm{v}}} \\ & \times \sum_{J=0}^{J_\mathrm{max}}(2J+1)e^{-hc\frac{\bar{E}_\mathrm{rot}(n,J)}{k_\mathrm{B}T_\mathrm{r}}} \sum_{v=0}^{v_\mathrm{max}} e^{-hc\frac{E_\mathrm{vib}(n,v)+E_\mathrm{inter}(n,v,J)-\mathcal{E}_0}{k_\mathrm{B}T_\mathrm{v}}}, \end{aligned} \tag{26}$$

respectively. The two-temperature internal energy $E_\mathrm{int}(T_\mathrm{v}, T_\mathrm{r})$ is written as:

$$E_\mathrm{int}(T_\mathrm{v}, T_\mathrm{r}) = R\left[T_\mathrm{v}^2\,\frac{\partial \ln Q_\mathrm{int}(T_\mathrm{v}, T_\mathrm{r})}{\partial T_\mathrm{v}} + T_\mathrm{r}^2\,\frac{\partial \ln Q_\mathrm{int}(T_\mathrm{v}, T_\mathrm{r})}{\partial T_\mathrm{r}}\right]. \tag{27}$$

One can note that when $T_r = T_v$, the previous expression reduces to Eq. 19. Vibrational and rotational contributions to the specific heat are defined from $E_{int}(T_v, T_r)$ partial derivatives by:

$$C_P^{vib}(T_v, T_r) = \frac{\partial E_{int}(T_v, T_r)}{\partial T_v}, \tag{28}$$

$$C_P^{rot}(T_v, T_r) = \frac{\partial E_{int}(T_v, T_r)}{\partial T_r}. \tag{29}$$

Furthermore, at equilibrium, the internal specific heat is equal to the sum of the vibrational and rotational contributions:

$$C_{p,int}(T) = C_P^{vib}(T_v = T, T_r = T) + C_P^{rot}(T_v = T, T_r = T). \tag{30}$$

3.2 Nonequilibrium Results and Discussion

The sensitivity of the thermodynamic functions to the choice of the energy partitioning scheme has been investigated and is presented here for the two main diatomic species, CO and O_2, encountered in CO_2 plasmas. Contour plots of the two-temperature partition functions are shown in Fig. 5 versus rotational T_r and vibrational T_v temperatures for the two energy partitioning schemes defined, respectively, by Eq. 25 (E_{inter} associated with T_r) and Eq. 26 (E_{inter} associated with T_v). These two partitioning schemes are referenced hereafter, respectively, as models (i) and (ii). Since the interaction term E_{inter} is generally negative, it can be observed that the partition function calculated according to scheme (i) is greater (respectively lower) than the one obtained with scheme (ii) for T_r greater (respectively lower) than T_v. The sign of E_{inter} also explains the behavior observed on contour plots of the dimensionless internal energy, defined by

$$\widehat{E}_{int} = \frac{E_{int}(T_v, T_r)}{\sqrt{T_r T_v}}, \tag{31}$$

and shown in Fig. 6. Deviations observed between the two models for both partition functions and internal energies obviously increase with the departure from equilibrium (i.e., with $|T_v - T_r|$) but do not exceed 8% for $|T_v - T_r| < 8{,}000$ K. However, the deviations for internal energies do not increase symmetrically versus T_v and T_r with departure from equilibrium: they even remain very small (lower than 5%) for strong thermal nonequilibrium corresponding to high T_v and low T_r values, while for strong nonequilibrium corresponding to low vibrational temperatures (<10,000 K) and high rotational ones, they may reach 15% for T_r about 30,000 K. This asymmetrical behavior may be explained by the higher electronic and vibrational energy contributions compared to the rotational ones.

Figures 7 and 8 show comparisons between vibrational and rotational specific heats, respectively, calculated according to the two partitioning schemes. Large discrepancies of about 30–40% may be observed between the results of the two partitioning models at high temperature, particularly in the case of the rotational specific heat. The discrepancies observed for the vibrational specific heat are smaller (<5%) insofar as the interaction energies remain smaller than the mean vibrational energies; the major

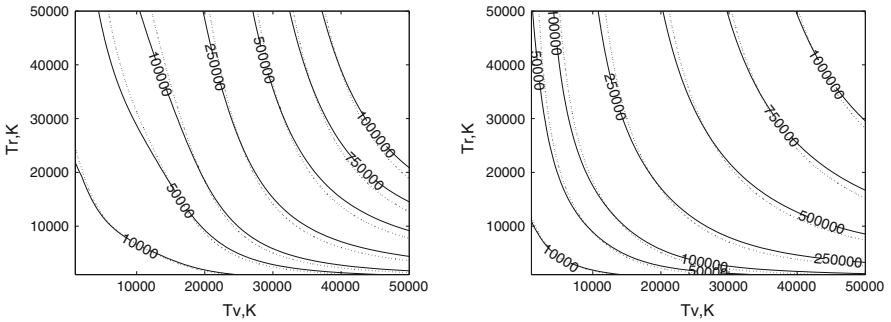

Fig. 5 Contour plot of the two-temperature partition function of CO (*left*) and O_2 (*right*) molecules versus vibrational (T_v) and rotational (T_r) temperatures as evaluated according to the two energy partitioning schemes defined respectively by Eq. 25 (*dotted lines*) and by Eq. 26 (*solid lines*)

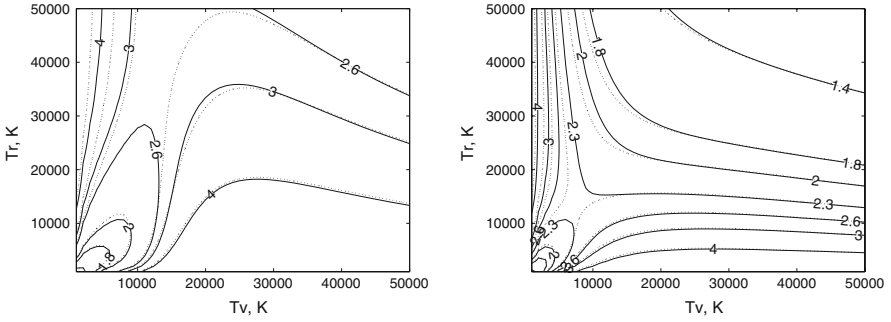

Fig. 6 Contour plots of two-temperature dimensionless internal energy $\widehat{E}_{\text{int}}$ (see Eq. 31) of CO (*left*) and O_2 (*right*) molecules versus vibrational (T_v) and rotational (T_r) temperatures as evaluated according to the two energy partitioning schemes (same conventions as in Fig. 5)

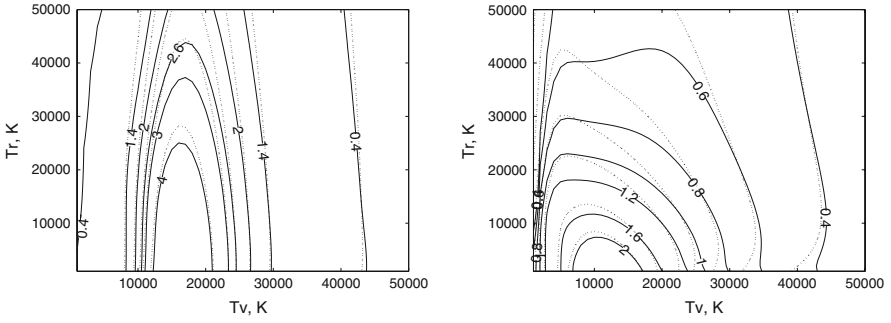

Fig. 7 Contour plots of the dimensionless specific heat vibrational contribution C_p^{vib}/R of CO (*left*) and O_2 (*right*) as evaluated according to the two energy partitioning schemes (same conventions as in Fig. 5)

discrepancies occur in this case at low vibrational and high rotational temperatures. Figure 8 shows that, in the case of the O_2 molecule, the rotational specific heat may become negative at large T_v and low T_r values. This behavior was already pointed out by Jaffe [10]. We have checked that this result is due to the vibrational energy contribution to the rotational specific heat:

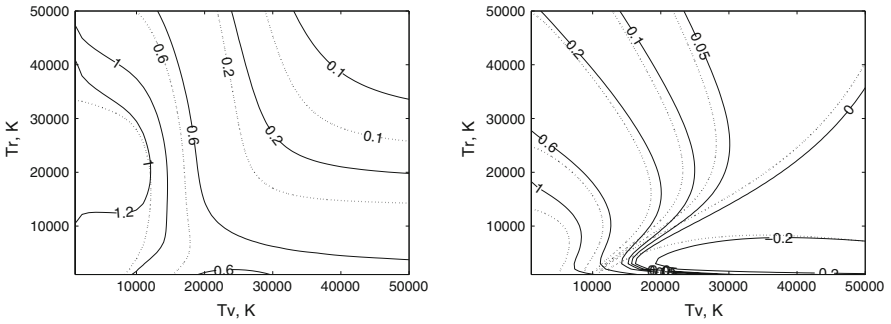

Fig. 8 Contour plots of the dimensionless specific heat rotational contribution C_p^{rot}/R of CO (*left*) and O_2 (*right*) as evaluated according to the two energy partitioning schemes (same conventions as in Fig. 5)

$$C_{P\,\mathrm{vib}}^{\mathrm{rot}} = \frac{\partial}{\partial T_{\mathrm{r}}}\left(RT_{\mathrm{v}}^2 \frac{\partial \ln Q_{\mathrm{int}}(T_{\mathrm{v}}, T_{\mathrm{r}})}{\partial T_{\mathrm{v}}}\right) \tag{32}$$

which is negative for both O_2 and CO molecules. This behavior is probably explained by observing that as T_{rot} increases, the contribution of higher rotational levels to the partition function increases. These higher rotational levels are associated with lower vibrational levels because of dissociation; this leads to a decrease of the average vibrational energy.

The thermodynamic data, computed from 1,000 to 50,000 K using the two partitioning schemes, are available upon request to the corresponding author.

4 Concluding Remarks

In this work, we have implemented up-to-date sets of spectroscopic data to generate partition functions and some thermodynamic functions of diatomic molecules at high temperatures or in thermal nonequilibrium. Calculations for N_2, O_2, CO, NO, CO, CN, C_2, N_2^+, and CO^+ have been carried out using direct summations over energy levels up to dissociation limit. For high temperature equilibrium, comparisons with available data have shown important sensitivity to the treatment of high-lying energy levels and to cutoff criteria. Reasonable agreement was however found for the most common molecules (N_2, O_2, CO). For nonequilibrium applications, we have generated partition functions, average energies and specific heats in the framework of a two-temperature description of the thermodynamic state. At high temperatures, an important effect of the vibration–rotation interaction energy is observed, especially on specific heats. Depending on its association with the vibrational/electronic or with the rotational/translational temperature, differences of computed rotational specific heats up to 40% have been observed for high rotational and low vibrational temperatures. The differences for average energies are limited to about 5%. These differences show clearly the inadequacy of approximate models such as harmonic oscillator and rigid rotor models, and outline the necessity of using consistent models for flow field calculations.

Appendix A: Spectroscopic Data

Table A1 Spectroscopic constants for the O_2 molecule (cm^{-1})

Electronic state	$X^3\Sigma_g^-$	$a^1\Delta_g$	$b^1\Sigma_g^+$	$c^1\Sigma_u^-$	$C^3\Delta_u$	$A^3\Sigma_u^+$	$^5\Pi$	$B^3\Sigma_u^-$	$2^3\Sigma_g^+$
T_e	0.0	7918.1	13195.1	33057.3	34690.0	35397.8	39279.0	49793.3	54031.0
ω_e	1580.1932	1483.5	1432.77	794.29	850.0	799.07	200.0	709.0577	537.0
$\omega_e x_e$	11.980804	12.9	14.0	12.736	20.0	12.16		10.614080	13.73
$\omega_e y_e$	0.047474736			−0.244		−0.550		−0.059212435	
$\omega_e z_e$	$-0.1272748 \times 10^{-2}$			0.5×10^{-3}				$-0.23974994 \times 10^{-1}$	
$\omega_e a_e$								2.2067951×10^{-3}	
$\omega_e b_e$								$-1.5990957 \times 10^{-4}$	
$\omega_e c_e$								4.4274814×10^{-6}	
B_e	1.445622	1.4264	1.40037	0.915	0.96	0.9106	0.53	0.818975	0.49
α_e	0.01593268	0.171×10^{-1}	0.182×10^{-1}	0.139×10^{-1}	0.26×10^{-1}	0.141×10^{-1}		−0.0119225	
γ_e	6.406456×10^{-5}							6.30472×10^{-4}	
δ_e	-2.846158×10^{-6}							1.57426×10^{-6}	
ϵ_e								6.70586×10^{-6}	
ξ_e								-9.35318×10^{-7}	
η_e								2.901×10^{-8}	
D_e	4.839×10^{-6}	4.86×10^{-6}	5.351×10^{-6}	7.4×10^{-6}		4.7×10^{-6}		4.55×10^{-6}	
E_{diss}	42048.0	34130.0	28852.9	8991.0	7358.0	6651.0	2769.0	8556.5	3806.7
Reference	[16]	[14]	[14]	[14]	[14]	[14]	[17]	[18]	[17]

	$2^3\Pi_g$	$3^3\Pi_g$	$^{1,3}\Pi_g$ [a]	$^{1,3}\Delta_u$ [a]	$2^1\Delta_g$	$^1\Phi_g$	$D^3\Sigma_u^+$	$f^1\Sigma_u^+$	$E^3\Sigma_u^-$	$^1\Sigma_u^+$
T_e	55524.0	57041.0	67841.0	69123.0	72842.0	74866.0	75260.0	76091.0	79883.0	82166.0
ω_e	221.0	200.0	1626.4	705.6	499.5	200.0	1957.0	1927.0	2547.0	792.4
$\omega_e x_e$			163.7	9.6	13.5		19.7	19.0		7.7
B_e	0.7117	0.5706	0.819	0.788	0.547	0.5259	1.73	1.703	1.4638	0.811
α_e			0.388×10^{-1}	0.101×10^{-1}	0.102×10^{-1}		0.25×10^{-1}	-0.2×10^{-1}		-0.92×10^{-2}
E_{diss}	2637.0	1186.0	8961.0	7299.0	3525.0	1581.0	22101.0	21270.0	17478.0	13333.0
Reference	[17]	[17]	[17]	[17]	[17]	[17]	[14]	[14]	[14]	[17]

[a] Two electronic states with identical spectroscopic constants were combined as a single state with a larger g_e

Table A2 Spectroscopic constants for the N_2^+ molecule (cm^{-1})

Electronic state	$X^2\Sigma_g^+$	$A^2\Pi_u$	$B^2\Sigma_u^+$	$a^4\Sigma_u^+$	$^4\Pi_g$	$^4\Delta_u$	$D^2\Pi_g$	$^4\Sigma_u^-$
T_e	0.0	9167.46	25461.11	25467	41940.5	45973.23	52318.2	53232.16
ω_e	2207.22	1903.7	2421.14	2398.00	1110	1110	911.7	1342
$\omega_e x_e$	16.226	15.111	24.07	14.0			12.606	
$\omega_e y_e$	4×10^{-3}	1.12×10^{-2}	-30×10^{-2}					
$\omega_e z_e$	-6.1×10^{-3}	-0.27×10^{-3}	-66.7×10^{-3}					
$\omega_e a_e$	3.9×10^{-4}							
$\omega_e b_e$	-1.4×10^{-5}							
$\omega_e c_e$	2×10^{-7}							
B_e	1.93171	1.7445	2.08507	2.071		1.04	1.113	1.26
α_e	1.8816×10^{-2}	1.87×10^{-2}	2.12×10^{-2}	0.14×10^{-1}		1.25	0.02	
γ_e	-6.77×10^{-5}	-0.6×10^{-4}	-5×10^{-4}					
δ_e	-2.32×10^{-6}	-0.11×10^{-5}	-8.8×10^{-5}					
D_e	5.92×10^{-6}							
β_e	3.9×10^{-8}							
E_{diss}	71368.0	62352.0	45799.0	45901.0	26616	39521	19204.5	32261.0
Reference	[19]	[19]	[19]	[14]	[20]	[20]	[14]	[20]

Electronic state	$^4\Sigma_u^+$	$^4\Pi_u$	$^4\Delta_g$	$^2\Delta_u$	$C^2\Sigma_u^+$	$^2\Pi_g$	$^2\Sigma_u^-$	$^4\Sigma_g^-$
T_e	57264.9	60491.09	62104.2	63717.28	64609.053	65330.4	67000.0	72000
ω_e	851	783	937.0	1190	2069.4	682	1022	926
$\omega_e x_e$					8.3			
$\omega_e y_e$					0.160×10^{-1}			
B_e	0.93	0.71	0.88	1.21	1.5098	1.06	1.28	0.88
α_e					1×10^{-3}			
E_{diss}	10485	6452.4	6452.4	31455	26057.15	29842.3	29035	12900
Reference	[20]	[20]	[20]	[20]	[19]	[20]	[20]	[20]

Table A3 Spectroscopic constants for the N_2 molecule (cm^{-1})

Electronic state	$X^1\Sigma_g^+$	$A^3\Sigma_u^+$	$B^3\Pi_g$	$W^3\Delta_u$	$B'^3\Sigma_u$	$A'^1\Sigma_u^-$	$A^1\Pi_g$	$W^1\Delta_u$	$^5\Sigma_g^+$	$g^3\Delta_g$	$C^3\Pi_u$
T_e	0.0	50203.6	59619.3	59808.0	66272.4	68152.7	69283.1	72097.4	76436.0	87900.0	89136.9
ω_e	2358.56	1460.94	1734.025	1506.5	1516.60	1530.25	1694.20	1559.26	667.00	742.49	2047.79
$\omega_e x_e$	14.317	13.98	14.412	12.5	12.0	12.075	13.949	11.63		11.85	28.942
$\omega_e y_e$	-0.331×10^{-2}	0.24×10^{-1}	-0.33×10^{-2}								0.225×10
$\omega_e z_e$	-0.195×10^{-3}	-0.256×10^{-2}	-0.79×10^{-3}								-0.551
$\omega_e a_e$			4.2×10^{-5}								
$\omega_e b_e$			1.68×10^{-6}								
B_e	1.998236	1.4539	1.63772	1.47	1.473	1.4799	1.6169	1.498	0.921	0.928	1.8268
α_e	$0.17309863 \times 10^{-1}$	0.175×10^{-1}	0.1793×10^{-1}	0.171×10^{-1}	0.166×10^{-1}	0.1657×10^{-1}	0.1793×10^{-1}	0.166×10^{-1}		0.161×10^{-1}	0.24×10^{-1}
γ_e	-3.01203×10^{-5}	-1.4×10^{-4}	-1.0×10^{-4}								1.9×10^{-3}
δ_e	-6.927×10^{-8}		5.0×10^{-6}								-6.0×10^{-4}
ϵ_e			2.1×10^{-7}								
D_e	5.73729×10^{-6}	5.46×10^{-6}	5.88×10^{-6}		5.56×10^{-6}	5.55×10^{-6}	5.89×10^{-5}				5.1×10^{-6}
β_e	0.8951×10^{-8}	0.11×10^{-6}	0.13×10^{-7}								0.22×10^{-5}
g_e	1.8×10^{-10}										-0.13×10^{-5}
h_e											2.4×10^{-7}
E_{diss}	79886.6	30135.8	39811.7	39301.0	42452.0	50181.0	49051.0	46237.0	3448.0	11209.0	10140.7
Reference	[21]	[22]	[22]	[23]	[14]	[14]	[14]	[14]	[24]	[14]	[25]

Table A4 Spectroscopic constants for the NO molecule (cm^{-1})

Electronic state	$X^2\Pi$	$a^4\Pi$	$A^2\Sigma^+$	$B^2\Sigma^+$	$b^4\Sigma^-$	$C^2\Pi$	$D^2\Sigma^+$	$L'^2\Phi$
T_e	0.0	38807.0	43965.7	45932.3	47950.0	52179.8	53084.7	53637.0
ω_e	1904.13	1019.00	2374.31	1042.40	1206.0	2381.3	2323.9	1004.4
$\omega_e x_e$	14.088358	12.800	16.106	7.7726	15.000	15.702	22.885	11.0
$\omega_e y_e$	0.0100467		-0.465×10^{-1}	0.11596			0.75	
$\omega_e z_e$	-1.5331×10^{-4}			-3.9577×10^{-3}			-0.22	
$\omega_e a_e$	-9.769×10^{-6}							
$\omega_e b_e$	-1.9142×10^{-7}							
$\omega_e c_e$	-5.2734×10^{-9}							
B_e	1.70488847	1.1275	1.9965	1.1244	1.3358	2.0155	2.0026	1.1275
α_e	0.01754158		0.1915×10^{-1}	0.13433×10^{-1}		3.244×10^{-2}	0.2175×10^{-1}	
γ_e	-1.4886×10^{-5}			2.991×10^{-5}				
δ_e				-3.177×10^{-6}				
ϵ_e	-4.7275×10^{-8}							
ξ_e	1.0108×10^{-9}							
η_e	-6.0557×10^{-11}							
D_e	5.46600×10^{-6}		5.4×10^{-6}	5.2×10^{-6}		5.8×10^{-6}	5.9×10^{-6}	
β_e	0.170320×10^{-7}			1.4×10^{-8}		1.8×10^{-8}	5.9×10^{-8}	
E_{diss}	53344.0	14537.0	28603.0	26637.0	21184.0	20383.0	19484.0	18932.0
Reference	[26]	[27]	[14]	[28]	[27]	[28]	[14]	[29]

Electronic state	$B'^2\Delta$	$E^2\Sigma^+$	$F^2\Delta$	$H^2\Sigma^+$	$H'^2\Sigma^+$	$G^2\Sigma^-$	$L^2\Pi$	$K^2\Pi$
T_e	60364.2	60628.8	61800.0	62473.4	62485.4	62913.0	63040.4	64077.5
ω_e	1217.4	2375.3	2394.0	2339.4	2371.3	1085.54	952.0	2438.3
$\omega_e x_e$	15.610	16.43	20.0		16.17	11.083	11.280	48.380
$\omega_e y_e$						-0.144		
B_e	1.332	1.9863	1.982	2.003	2.015	1.2523	1.132	2.034
α_e	0.21×10^{-1}	0.182×10^{-1}	0.23×10^{-1}	0.18×10^{-1}	0.21×10^{-1}	0.204×10^{-1}	0.221×10^{-1}	0.56×10^{-1}
D_e		5.6×10^{-6}						
E_{diss}	12205.0	11940.0	10769.0	10096.0	86936.0	9656.0	19144.0	18106.0
Reference	[30]	[14]	[14]	[14]	[14]	[14]	[28]	[28]

Table A5 Spectroscopic constants for the C_2 molecule (cm^{-1})

Electronic state	$X^1\Sigma_g^+$	$a^3\Pi_u$	$b^3\Sigma_g^-$	$A^1\Pi_u$	$c^3\Sigma_u^+$	$B^1\Delta_g$	$B'^1\Sigma_g^+$	$d^3\Pi_g$	$^5\Pi_g$	$^5\Sigma_g^+$
T_e	0.0	716.2	6434.8	8391.3	9124.2	12082.3	15409.1	20022.5	22485.0	30474.0
ω_e	1855.01	1641.35	1470.41	1608.22	2085.9	1407.47	1424.12	1788.22	1400	1550
$\omega_e x_e$	13.555	11.670	11.155	12.055	18.623	11.479	2.571	16.457		
$\omega_e y_e$	−0.132		0.139×10^{-1}	-0.120×10^{-1}		0.103×10^{-1}	0.46398	−0.501		
$\omega_e z_e$	0.357×10^{-2}									
$\omega_e a_e$	−0.001116									
B_e	1.820099	1.632400	1.498643	1.616477	1.921000	1.463685	1.481006	1.755234	1.8[a]	1.8[a]
α_e	0.1801×10^{-1}	0.1661×10^{-1}	0.1631×10^{-1}	0.1687×10^{-1}	0.1255×10^{-1}	0.0168161	-0.1175×10^{-1}	0.1907×10^{-1}		
γ_e	-6.33×10^{-5}		-0.461×10^{-5}	-5.47×10^{-5}		-1.503×10^{-5}	67.18×10^{-5}	-0.535×10^{-3}		
δ_e	-2.06×10^{-6}									
D_e	6.964×10^{-6}	6.44×10^{-6}	6.19577×10^{-6}	6.494×10^{-6}				6.74×10^{-6}		
β_e	6.41×10^{-8}		0.00662×10^{-6}	0.3×10^{-7}						
g_e			0.000478×10^{-6}							
E_{diss}	50247.9	49531.7	43812.2	41866.7	37988.4	31858.6	28531.2	30225.4	13711.3	20567.0
Reference	[31]	[32]	[33]	[34]	[35]	[36]	[36]	[37]	[38]	[38]

Electronic state	$C^1\Pi_g$	$C'^1\Pi_g$	$^1\Sigma_u^-$	$e^3\Pi_g$	$^3\Delta_u$	$D^1\Sigma_g^+$	$E^1\Sigma_g^+$	$f^3\Sigma_g^-$	$g^3\Delta_g$	$F^1\Pi_u$
T_e	34261.9	39365.0	40012.84	40796.7	41117.81	43239.8	55034.7	71045.8	73183.6	75456.9
ω_e	1809.1	1697.0	724.8	1106.56	721.2	1829.57	1671.5	1360.5	1458.06	1557.5
$\omega_e x_e$	15.81			39.26		13.94	40.02	14.8		
$\omega_e y_e$				2.81			0.248			
$\omega_e z_e$				−0.127						
B_e	1.7834	1.7113	0.9447	1.1922	0.9421	1.8332	1.793	1.448	1.5238	1.645
α_e	0.18×10^{-1}	0.43×10^{-1}		0.242×10^{-1}		0.196×10^{-1}	0.0421	0.4	0.017	0.019
γ_e							−0.0005			
D_e		1.13×10^{-5}		6.3×10^{-6}		7.32×10^{-6}	8.3×10^{-6}	10×10^{-6}	6.6×10^{-6}	
β_e							0.6×10^{-6}			
E_{diss}	15986.6	10565.8	10766	19643.9	9634	39843.5	16861.2	39535.55	37535.55	35124.45
Reference	[14]	[39]	[40]	[41]	[40]	[14]	[14]	[14]	[14]	[14]

[a] Arbitrary value

Table A6 Spectroscopic constants for the CN molecule (cm^{-1})

Electronic state	$X^2\Sigma^+$	$A^2\Pi_i$	$B^2\Sigma^+$	$a^4\Sigma^+$	$b^4\Pi$	$c^4\Delta$	$d^4\Sigma^-$	$D^2\Pi_i$	$E^2\Sigma^+$
T_e	0.0	9240.0	25752.0	32390	42956	47690	53716	54486.0	59151.2
ω_e	2068.65	1813.26	2161.46	1249.4	873.0	1274.4	1286.0	1004.7	1681.43
$\omega_e x_e$	13.097	12.7687257	18.219	14.82	13.15	14.82	15.36	8.78	3.6
$\omega_e y_e$	-0.124×10^{-1}	$-0.356900772 \times 10^{-2}$	−0.486						−1.02
$\omega_e z_e$	0.700×10^{-3}	$0.107074461 \times 10^{-3}$	0.4×10^{-1}						
$\omega_e a_e$	-0.323×10^{-4}	$-0.466480810 \times 10^{-5}$	-6.93×10^{-3}						
$\omega_e b_e$		$-0.252730323 \times 10^{-6}$	4.32×10^{-4}						
$\omega_e d_e$			-8.34×10^{-6}						
B_e	1.899783	1.71590743	1.96891	1.174	0.927	1.184	1.177	1.162	1.4871
α_e	0.1737×10^{-1}	0.0171673224	2.0337×10^{-2}	0.0152	0.0154	0.0147	0.0138	0.013	0.643×10^{-2}
γ_e	-0.2586×10^{-4}	$-5.49049968 \times 10^{-5}$	-5.9×10^{-5}						−0.00077
δ_e	-0.211×10^{-6}	$0.675937372 \times 10^{-5}$	-7.71×10^{-5}						
ϵ_e	-0.161×10^{-7}	$-0.588512508 \times 10^{-6}$	3.1×10^{-6}						
ξ_e		$0.189044134 \times 10^{-7}$							
η_e		$-0.234754466 \times 10^{-9}$							
D_e								7.0×10^{-6}	5.0×10^{-6}
E_{diss}	63296.6	54053.3	56777.0	17437.6	6880	17639	11453	24261	14074
Reference	[42]	[43]	[44]	[45]	[45]	[45]	[45]	[46]	[14]

Electronic state	$F^2\Delta_r$	$H^2\Pi_r$	$G^2\Phi$	$^2\Sigma^-$	$J^2\Delta_i$	$^4\Delta$	$^2\Sigma^-$
T_e	60095.64	62967.2	62442	64427	65258.19	69516	70200
ω_e	1239.5	1651.3	950.70	1225.5	1121.76	651.5	1183.2
$\omega_e x_e$	12.75	43.84	12.63	14.92	14.203	2.75	14.04
$\omega_e y_e$					0.18		
B_e	1.3834	1.229	0.936	1.165	1.305	0.77	1.142
γ_e	0.0187	0.0021	0.0123	0.0155	0.0208	0.0057	0.0157
D_e	7×10^{-6}				5.8×10^{-6}		
E_{diss}	13888.8	14469	15000	13010	9428.5	7920	16777
Reference	[14]	[45]	[45]	[45]	[14]	[45]	[45]

Table A7 Spectroscopic constants for the CO molecule (cm^{-1})

Electronic state	$X^1\Sigma^+$	$a^3\Pi_r$	$a'^3\Sigma^+$	$d^3\Delta$	$^5\Pi$	$e^3\Sigma^-$	$A^1\Pi$	$I^1\Sigma^+$	$D^1\Delta$
T_e	0.0	48686.8	55825.49	61120.1	62507.5	64230.2	65075.8	65084.4	65928.0
ω_e	2169.812670	1743.41	1228.60	1171.94	759.00	1117.72	1518.24	1092.22	1094.0
$\omega_e x_e$	13.28787634	14.36	10.466	10.635	25.2	10.686	19.4	10.704	10.2
$\omega_e y_e$	$0.1041106647 \times 10^{-1}$	-0.45×10^{-1}	0.0091	0.0785			0.76584	0.554×10^{-1}	
$\omega_e z_e$	$0.6936640756 \times 10^{-4}$	-0.25×10^{-2}	-0.259×10^{-2}	−0.00163			−0.14117	0.108×10^{-2}	
$\omega_e a_e$	$0.1679352306 \times 10^{-6}$						1.434×10^{-2}		
$\omega_e b_e$	$0.2059251576 \times 10^{-8}$						-8.051×10^{-4}		
$\omega_e c_e$	$-0.8488145707 \times 10^{-9}$						2.36×10^{-5}		
$\omega_e d_e$	$0.1238772013 \times 10^{-10}$						-2.90×10^{-7}		
$\omega_e e_e$	$-0.8233737278 \times 10^{-13}$								
B_e	1.931280985	1.691240	1.344600	1.3108	0.931	1.2836	1.6115	1.2705	1.257
α_e	$0.1750439229 \times 10^{-1}$	0.1904×10^{-1}	0.1892×10^{-1}	0.01782	0.0231	0.1753×10^{-1}	0.23251×10^{-1}	0.1848×10^{-1}	0.17×10^{-1}
γ_e	$0.7173917007 \times 10^{-6}$	-4.1×10^{-5}		0.000113		7.0×10^{-6}	1.5911×10^{-3}		
δ_e	$-0.2146354586 \times 10^{-7}$						-5.7160×10^{-4}		
ϵ_e	$0.4435403909 \times 10^{-8}$						8.2417×10^{-5}		
ξ_e	$-0.1361069450 \times 10^{-9}$						-5.9413×10^{-6}		
η_e	$0.1245785715 \times 10^{-11}$						2.1149×10^{-7}		
θ_e	$-0.2125123415 \times 10^{-13}$						-2.991×10^{-9}		
D_e	$6.121615183 \times 10^{-6}$	6.36×10^{-6}	6.41×10^{-6}	6.59×10^{-6}		6.77×10^{-6}	7.29×10^{-6}	9.0×10^{-6}	
β_e	$-0.1034922952 \times 10^{-8}$	0.04×10^{-6}							
g_e	$0.1849766981 \times 10^{-9}$								
h_e	$-0.2431110877 \times 10^{-11}$								
k_e	$0.1043488564 \times 10^{-12}$								
E_{diss}	90575.3	41888.6	34842.9	29519.6	3548.81	27422.6	25499.6	25567.5	25000
Reference	[47]	[48]	[14]	[14]	[49]	[14]	[50]	[51]	[14]

Table A8 Spectroscopic constants for the CO^+ molecule (cm^{-1})

Electronic state	$X^2\Sigma^+$	$A^2\Pi_i$	$a^4\Sigma^+$	$B^2\Sigma^+$	$^4\Delta$	$b^4\Pi$	$^4\Sigma$	$C^2\Delta$
T_e	0	20733.3	45857	45876.7	54063	56340	58773	63012.0
ω_e	2214.13	1567.81	1405.6	1734.57	1274.0	495.1	1096.2	1144.0
$\omega_e x_e$	15.094	13.479	20.01	28.248	30.74	5.02	34.24	33.3
$\omega_e y_e$	-0.117×10^{-1}	0.865×10^{-2}		0.399				
B_e	1.977200	1.5894	1.8[a]	1.7999	1.8[a]	1.8[a]	1.8[a]	1.357
α_e	0.1896×10^{-1}	0.1942×10^{-1}		0.3025×10^{-1}				0.24×10^{-1}
D_e	6.35×10^{-6}	6.6×10^{-6}		7.75×10^{-5}				
E_{diss}	68288.8	47556.8	47876.8	38279.6	13879.3	11567.3	9274.5	5626.7
Reference	[52]	[52]	[15]	[53]	[15]	[15]	[15]	[14]

[a] Arbitrary value

References

1. S. Chauveau, M.-Y. Perrin, Ph. Rivière, A. Soufiani, J. Quant. Spectrosc. Radiat. Transf. **72**, 503 (2002)
2. J.H. Lee, AIAA Progress in Astronautics and Aeronautics: Thermal Design of Aeroassisted Transfer Vehicles **96**, 3 (1985)
3. C. Park, AIAA Progress in Astronautics and Aeronautics: Thermophysical Aspect of Re-entry Flows **103**, 478 (1986)
4. C. Park, in *Proc. 4th AIAA and ASME Joint Thermophys. Heat Transfer Conf.*, Boston (1986), AIAA paper 1986–1347
5. M.W. Chase Jr., C.A. Davies, J.R. Downey Jr., D.J. Frurip, R.A. McDonald, A.N. Syverud, J. Phys. Chem. Ref. Data **14**, 1 (1985)
6. B.J. Mac Bride, M.J. Zehe, S. Gordon, NASA Glenn Coefficients for Calculating Thermodynamic Properties of Individual Species, NASA Tech. Paper 2002-211556 (2002)
7. L.V. Gurvich, I.V. Veyts, C.B. Alcock, *Thermodynamic Properties of Individual Substances*, vol. 1, 4th edn. (Hemisphere, New York, 1991)
8. L.V. Gurvich, I.V. Veyts, C.B. Alcock, *Thermodynamic Properties of Individual Substances*, vol. 2, 4th edn. (Hemisphere, New York, 1989)
9. M. Capitelli, G. Colonna, D. Giordano, L. Marraffa, A. Casavola, P. Minelli, D. Pagano, L.D. Pietanza, F. Taccogna, B. Warmbein, Tables of Internal Partition Functions and Thermodynamic Properties of High-Temperature Mars-Atmosphere Species from 50 K to 50000 K, ESA Scientific Technical Review 246 (2005)
10. R.L. Jaffe, in *Proc. 22nd AIAA Thermophys. Conf.*, Honolulu (1987), AIAA paper 1987–1633
11. K.S. Drellishak, D.P. Aeschliman, A.B. Cambel, Phys. Fluids **8**, 1590 (1965)
12. Y. Liu, F. Shakib, M. Vinokur, Phys. Fluids A: Fluid Dynam. **2**, 1884 (1990)
13. G. Herzberg, *Molecular Spectra and Molecular Structure. Spectra of Diatomic Molecules* (D. Van Nostrand Reinhold Company, Inc., New-York, 1950)
14. K.P. Huber, G. Herzberg, *Molecular Spectra and Molecular Structure. Constants of Diatomic Molecules* (D. Van Nostrand Reinhold Company, Inc., New-York, 1979)
15. K. Okada, S. Iwata, J. Chem. Phys. **112**, 1804 (2000)
16. D.L. Albritton, A.L. Schmeltekopf, R.N. Zare, unpublished results, cited in C.O. Laux, Ph.D. Thesis (Stanford University, Report T-288, 1993)
17. R.P. Saxon, B. Liu, J. Chem. Phys. **67**, 5432 (1977)
18. A.S.C. Cheung, K. Yoshino, W.H. Parkinson, D.E. Freeman, J. Mol. Spectrosc. **119**, 1 (1986)
19. L. Klynning, P. Pages, Phys. Scripta **25**, 543 (1982)
20. E.W. Thulstrup, A. Andersen, J. Phys. B: At. Mol. Opt. Phys. **8**, 965 (1975)
21. S. Edwards, J.Y. Roncin, F. Launay, F. Rostas, J. Mol. Spectrosc. **162**, 257 (1993)
22. F. Roux, F. Michaud, Can. J. Phys. **68**, 1257 (1990)
23. H.J. Werner, J. Kalcher, E.A. Reinsch, J. Chem. Phys. **81**, 2420 (1984)
24. H. Partridge, C.W. Bausclisher Jr., unpublished, cited in Ref. [10]
25. F. Roux, F. Michaud, M. Vervloet, J. Mol. Spectrosc. **158**, 270 (1993)
26. C. Amiot, J. Mol. Spectrosc. **94**, 150 (1982)
27. H. Partridge, S.R. Langhoff, unpublished, cited in Ref. [10]
28. R. Galluser, K. Dressler, J. Chem. Phys. **76**, 4311 (1982)
29. M. Chergui, V. Chandrasekharan, W. Bohmer, R. Haensel, H. Wicke, N. Schwentner, Chem. Phys. Lett. **105**, 386 (1984)
30. Ch. Jungen, Can. J. Phys. **44**, 3197 (1966)
31. M. Douay, R. Nietmann, P.F. Bernath, J. Mol. Spectrosc. **131**, 250 (1988)
32. J.G. Phillips, S. P. Davis, *The Swan System of the C_2 Molecule* (University of California Press, Berkeley and Los Angeles, 1968)
33. C. Amiot, J.P. Maillard, J. Chauville, J. Mol. Spectrosc. **75**, 19 (1979)
34. R. Marenin, H.R. Johnson, J. Quant. Spectrosc. Radiat. Transf. **10**, 305 (1970)
35. J. Chauville, J.P. Maillard, A.W. Mantz, J. Mol. Spectrosc. **68**, 399 (1977)
36. M. Douay, R. Nietmann, P.F. Bernath, J. Mol. Spectrosc. **131**, 261 (1988)
37. C.V.V. Prasad, P.F. Bernath, Astrophys. J. **426**, 812 (1994)
38. P.F. Fougere, R.K. Nesbet, J. Chem. Phys. **44**, 285 (1966)
39. G. Messerle, L. Krauss, Zeitschrift für Naturforschung A Astrophysik Physik und Physikalische Chemie **22a**, 2015 (1967)

40. M. Boggio-Pasqua, A.I. Voronin, Ph. Halvick, J.-C. Rayez, J. Mol. Struct. (Theochem) **531**, 159 (2000)
41. J.G Phillips, Astrophys. J. **110**, 73 (1949)
42. C.V.V. Prasad, P.F. Bernath, J. Mol. Spectrosc. **156**, 327 (1992)
43. H. Ito, A. Kazama, K. Kuchitsu, J. Mol. Spectrosc. **324**, 29 (1994)
44. H. Ito, Y. Ozaki, T. Kondow, K. Kuchitsu, J. Mol. Spectrosc. **127**, 283 (1988)
45. H.F. Schaefer, T.G. Heil, J. Chem. Phys. **54**, 2573 (1971)
46. P.K. Carroll, Can. J. Phys. **34**, 83 (1956)
47. R. Farrenq, G. Guelachvili, A.J. Sauval, N. Grevesse, C.B. Farmer, J. Mol. Spectrosc. **149**, 375 (1991)
48. R.W. Field, S.G. Tilford, R.A. Howard, J.D. Simmons, J. Mol. Spectrosc. **44**, 347 (1972)
49. H.F. O'Neil, S.V. Schaefer, J. Chem. Phys. **53**, 3394 (1970)
50. J.D. Simmons, A.M. Bass, S.G. Tilford, Astrophys. J. **155**, 345 (1969)
51. S.G. Tilford, J.D. Simmons, J. Phys. Chem. Ref. Data **1**, 147 (1972)
52. R. Kepa, A. Kocan, M. Ostrowska-Kopec, I. Piotrowska-Domagala, M. Zachwieja, J. Mol. Spectrosc. **228**, 66 (2004)
53. U. Bembenek, Z. Domin, R. Kepa, M. Porada, K. Rytel, M. Zachwieja, Z. Jakubek, J.D. Janjic, J. Mol. Spectrosc. **165**, 205 (1994)